Europace (2008) **10**, 939–948
doi:10.1093/europace/eun147

Computed tomography model-based treatment of atrial fibrillation and atrial macro-re-entrant tachycardia

Christopher Piorkowski*, Simon Kircher, Arash Arya, Thomas Gaspar, Masahiro Esato, Sam Riahi, Andreas Bollmann, Daniela Husser, Charlotte Staab, Philipp Sommer, and Gerhard Hindricks

Department of Electrophysiology, University of Leipzig, Heart Center, Strümpellstrasse 39, 04289 Leipzig, Germany

Received 2 February 2008; accepted after revision 12 May 2008; online publish-ahead-of-print 23 June 2008

KEYWORDS
Atrial fibrillation;
Ablation;
Three dimensional image;
Model-guided therapy

Aims Accurate orientation within true three-dimensional (3D) anatomies is essential for the successful radiofrequency (RF) catheter ablation of atrial fibrillation (AF) and atrial macro-re-entrant tachycardia (MRT). In this prospective study, ablation of AF and MRT was performed exclusively using a pre-acquired and integrated computed tomography (CT) image for anatomical 3D orientation without electro-anatomic reconstruction of the left atrium (LA).

Methods and results Fifty-four consecutive patients suffering from AF ($n = 36$) and/or MRT ($n = 18$) underwent RF catheter ablation. A 3D CT image was registered into the NavX-Ensite system without reconstruction of the atrial chamber anatomy. The quality of CT alignment was assessed and validated according to fluoroscopy information, electrogram characteristics, and tactile feedback at 31 predefined LA control points. The ablation of AF as well as mapping and ablation of MRT was performed within the 3D CT anatomy. In all patients, mapping and ablation could be performed without the reconstruction of the respective atrial chamber anatomy. The overall CT alignment was highly accurate with true surface contact in 90% (84%; 100%) of the control points. Complete isolation of all pulmonary vein (PV) funnels was achieved in 35 of 36 patients (97%) with AF. In patients with persistent AF ($n = 11$), additional isolation of the posterior LA (box lesion) and the placement of a mitral isthmus line were performed. The MRT mechanisms were as follows: around a PV ostium ($n = 6$), perimitral ($n = 4$), through LA roof ($n = 5$), septal ($n = 2$), and around left atrial appendage ($n = 1$). After a follow-up of 122 ± 33 days, 22/25 (88%) patients with paroxysmal AF, 8/11 (73%) with persistent AF, and 16/18 (89%) with MRT remained free from arrhythmia recurrences.

Conclusion For patients with AF and MRT, our study shows the feasibility of successful placement of complex linear ablation line concepts guided by an integrated 3D image anatomy alone rather than catheter-based virtual chamber surface reconstructions.

Introduction

Radiofrequency (RF) catheter ablation of atrial fibrillation (AF) and atrial macro-re-entrant tachycardia (MRT) has become an accepted potentially curative treatment approach. Because of the complex three-dimensional (3D) distributions of initiating triggers and perpetuating substrate, catheter ablation of the mentioned arrhythmias requires an accurate 3D visualization of the atrial anatomy.

To provide 3D orientation, currently, electro-anatomic mapping systems (EAM) are commonly being used to reconstruct a virtual 3D chamber anatomy through the acquisition of a limited number of anatomical surface location points derived from the position of the catheter tip and an extrapolation of the chamber surface in between these acquired anatomical points.[1,2] However, the resolution and accuracy of such a virtual 3D chamber anatomy, solely based on EAM, are limited by the number of acquired anatomical surface location points and the reliability of a true surface location of the catheter tip in areas with difficult catheter access.

* Corresponding author. Tel: +49 341 8651413; fax: +49 341 8651460.
E-mail address: cp7026@yahoo.de

A more detailed appreciation of the complex left atrium (LA) anatomy can be obtained with 3D-anatomical chamber reconstructions derived from computed tomography (CT) or magnetic resonance imaging (MRI) studies.[3,4] Superimposition of pre-acquired CT/MRI images onto the electro-anatomic 3D-reconstruction is associated with an improved clinical outcome in AF ablation procedures.[5] So far this image integration is based on registration involving landmark points and surface alignment. Currently, it is not clear which registration protocol provides the most accurate and reliable image integration. Therefore, until now, CT/MRI imaging has been merely used in adjunction to the electro-anatomic reconstruction.

In the present prospective clinical study, ablation of AF and atrial MRT was performed in a larger patient population exclusively using a pre-acquired and integrated CT image for anatomical 3D orientation without electro-anatomic reconstruction of the LA.

Methods

Patient characteristics

In this prospective study, between May 2007 and September 2007, a total of 54 consecutive patients suffering from highly symptomatic drug-refractory AF ($n = 36$) and/or atrial MRT ($n = 18$) underwent RF catheter ablation at our institution (21 females, 33 males, mean age 61 $\pm$ 10 years). Out of the 36 patients with AF, 25 (69%) suffered from paroxysmal and 11 (31%) from persistent AF. Persistent AF was defined as documented AF lasting for more than 7 days.

Among 54 patients, structural heart disease was present in 23 (43%) patients [coronary artery disease ($n = 7$), dilated cardiomyopathy ($n = 8$), and valvular heart disease ($n = 9$)]. Arterial hypertension was present in 31 (57%) patients. Lone AF was seen in 13 (24%) patients. Left ventricular ejection fraction averaged 56 $\pm$ 9%. Left atrium diameter measured 44 $\pm$ 9 mm. The duration of the arrhythmia history had a median of 60 months (range: 8–252). Twenty-one of the 54 patients (39%) had undergone prior AF ablation procedures.

Table 1 displays baseline characteristics for the three groups of patients with paroxysmal AF, persistent AF, and atrial MRT separately.

Computed tomography imaging and segmentation

Forty of 54 (74%) patients received a cardiac CT imaging on a 64-slice helical system (Philips Brilliance 64 CT, Best, The Netherlands) as a standard imaging procedure within 24 h before electrophysiological study. For the remaining 14 (26%) patients, thoracic CT studies were used, which had been acquired previously, either for prior AF ablation procedures ($n = 13$) or for clinical indications other than electrophysiological therapy planning ($n = 1$).

Data acquisition was performed during expiratory breath hold in late diastole with the following scan parameters: effective thickness 0.8 mm, increment −0.8 mm, voltage 120 kV, tube current 500 mAs, rotation time 0.33 s, and scan time 16–20 s. Imaging was initiated at the transaxial level of the aortic arch and carried caudally to cover the cardiac chambers. Non-ionic-iodinated contrast material (Ultravist 370, Schering AG, Berlin, Germany) was administered intravenously (60 mL, 4 mL/s).

All CT data were uploaded onto the NavX-Ensite system (Endocardial Solutions, Inc., St Paul, MN, USA, version 7.0), by which segmentation and 3D reconstruction of the LA were performed using the incorporated segmentation software. The segmented anatomical 3D image was exported into the real-time mapping system for registration.

Electrophysiological study and registration process

Prior to the procedure, transoesophageal echocardiography was performed to exclude thrombus formation within the LA. Patients were studied under deep propofol sedation with continuous invasive monitoring of arterial blood pressure and oxygen saturation. Standard catheters were placed in the right ventricular apex and the coronary sinus.

Patients presenting with AF at the beginning of the procedure received an electrical cardioversion into sinus rhythm (SR). In patients presenting with an atrial MRT entrainment mapping within the high right atrium (RA), the RA isthmus and the coronary sinus confirmed the LA origin of the macro-re-entrant circuit.[6] A single trans-septal puncture was performed under fluoroscopic guidance to gain access to the LA. After trans-septal puncture, an initial intravenous bolus and repeated doses of heparin were administered to maintain an activated clotting time of 250–300 s. The NavX-Ensite system (Endocardial Solutions, Inc., St Paul, MN, USA, version 7.0) was used for non-fluoroscopic 3D catheter orientation, CT image integration, activation mapping, and tagging of the ablation sites with the coronary sinus lead 5/6 serving as system reference. Throughout the procedure, respiratory motion compensation of the NavX-EnSite system was used to stabilize the catheter image in the case of instability due to deep or changing breathing pattern. Trans-septal access and catheter navigation were performed with steerable sheath technology (Agilis, St Jude Medical, Inc., St Paul, MN, USA).

Computed tomography registration

For image integration, the 'Digital Image Fusion' (DIF) algorithm provided by NavX-EnSite (Endocardial Solutions, Inc., St Paul, MN, USA, version 7.0) was used. Among other features, DIF contains field scaling and morphing algorithms. Field scaling is designed to compensate for distortions in NavX anatomies caused by electrical field inhomogenities. Morphing artificially changes the NavX anatomy in order to improve the fit into a given 3D image. During our registration process, both these algorithms were intentionally not used.

A 7 Fr catheter containing a deflectable decapolar 4 Fr Lasso loop of variable diameter size (15–25 mm) (Optima, St Jude Medical, Inc., St Paul, MN, USA) was introduced into each pulmonary vein (PV) subsequently. Initial PV conduction was assessed. While backing out of each PV, anatomical points were acquired through all the 10 catheter poles simultaneously, using the automatic mode of anatomic point acquisition with the multipolar mapping catheter as 'Active EnGuide' (*Figure 1A*). The vein–atrium transition was determined combining information from the fluoroscopic cardiac silhouette, impedance changes, and PV–atrium electrogram characteristics. In this way, a separate anatomy for each of the four PVs was created (*Figure 1B*). These four PV anatomies served as the main anatomical structures for the integration of the CT image (*Figure 1C*). In order to align the Lasso-reconstructed PV anatomies with the CT-PVs, for each PV two to four anatomical landmarks were placed at corresponding locations between the NavX anatomy and the CT-PV surface. Care was taken to define the landmark on the NavX anatomy first and on the CT-PV second (and not vice versa), in order to bring the CT towards the NavX anatomy and to leave the morphology of the NavX anatomy itself unchanged (otherwise the morphing algorithm would have changed the NavX anatomy, which was not intended).

After the alignment of the Lasso-reconstructed PV anatomies with the CT-PVs, the multipolar mapping catheter was replaced by a 4 mm M-curve irrigated tip ablation catheter (IBI Therapy Cooled Path, St Jude Medical, Inc., St Paul, MN, USA). Further, fine adjustment of image integration was achieved through three additional landmarks (at the LA roof, at the basal posterior LA, and in the LA isthmus). These landmarks were visited with the ablation catheter tip according to fluoroscopy and electrogram information. Once the individual landmark was reached, the assumed corresponding

Table 1 Patient characteristics

	Paroxysmal AF ($n = 25$)	Persistent AF ($n = 11$)	MRT ($n = 18$)
Age (years)[a]	60 ± 8	62 ± 10	57 ± 15
Male, *n*(%)	15 (60)	7 (64)	11 (61)
AF/MRT history (months)[b]	60 (27; 108)	72 (18; 132)	72 (36; 111)
Arterial hypertension, *n*(%)	17 (68)	7 (64)	7 (39)
Coronary artery disease, *n*(%)	4 (16)	1 (9)	2 (11)
Dilated cardiomyopathy	0 (0)	1 (9)	7 (39)
Valvular heart disease, *n*(%)	1 (4)	2 (18)	6 (33)
Mitral valve replacement (*n*)	Mech. valve (1)	–	Mech. valve (4)
Mitral valve reconstruction (*n*)	–	Reconstruction (1)	Reconstruction (2)
Aortic valve replacement (*n*)	–	Mech. valve (1)	–
Lone AF, *n*(%)	9 (36)	2 (18)	2 (11)
Left atrial diameter (mm)[a]	37 ± 9	53 ± 6	47 ± 5
Left ventricular ejection fraction (%)[a]	64 ± 6	63 ± 7	50 ± 15
Prior AF ablation, *n*(%)	2 (8)	3 (27)	16 (89)

AF, atrial fibrillation and MRT, macro-re-entrant tachycardia.
[a]Data given as mean and standard deviation.
[b]Data given as median and quartiles.

position on the CT surface was marked and this way the CT surface was pulled towards the tip of the ablation catheter, without further anatomical point acquisition or anatomy reconstruction.

Assessment of alignment quality

After completion of the registration process, the quality of CT alignment was assessed through several LA control positions, which had to be visited with the ablation catheter by two electrophysiologists independently. Control point location and surface contact were reached and verified according to fluoroscopy information, electrogram characteristics, and tactile feedback. For each of the control points, the position of the catheter tip in relation to the integrated CT surface was evaluated in a nominal fashion.

The following control positions were visited: septal, inferior, posterior, and superior mitral annulus; LA isthmus; tissue bridge between left atrial appendage (LAA) and left upper pulmonary vein (LUPV); anterior, inferior, posterior, and superior wall of each PV; left-sided, middle, and right-sided LA roof; left-sided, middle, and right-sided basal LA; and annular, middle, and posterior part of the LA septum (*Figure 2*).

To further verify the quality of the image integration process, ablation points were not marked as projection onto the CT surface or as 'Lesion at Mouse', but they were taken as '3D Lesion on EnGuide' representing the true 3D anatomical position of the tip of the ablation catheter, demonstrating the presence or the absence of surface contact to the CT image.

Ablation procedure and follow-up

In all patients, an additional catheter was used for the reconstruction of the oesophageal anatomy (*Figure 3*). The oesophageal anatomy and location were stored in the map.[7]

For the treatment of paroxysmal AF, circumferential LA ablation lines were placed around the antrum of the ipsilateral PVs (irrigated tip catheter, pre-selected tip temperature of 48°C, and maximum power of 30–50 W) (*Figure 4A*). On the basis of reduction in the electrogram amplitude, the ablation catheter was moved to the next ablation position. Ablation in contact areas between the LA and the oesophagus was avoided. In regions near to the oesophagus, maximum power was reduced to 30 W, special attention was paid to local electrogram amplitude reduction, and the burning time was limited to 30 s. After circumferential line placement, voltage and pace mapping along the ablation line were used to identify and close gaps. The isolation of all PVs with bidirectional block was the procedural endpoint. This was additionally verified by the placement of a multipolar circular mapping catheter within the encircled areas, which was performed by a second electrophysiologist not involved in the ablation part of the procedure.

In patients with persistent AF, isolation of the PVs was performed after electrical cardioversion into SR, as described earlier. Additionally, linear lesions were added at the LA roof and the basal posterior LA, the latter always being placed with only 30 W due to oesophageal vicinity. Completeness of the additional linear lesions was achieved and verified through voltage and pace mapping within the isolated posterior LA box (*Figure 4B*). Eventually, an LA isthmus line was placed as continuous and transmural as possible, however, without line continuity enforcement through epicardial ablation. The ablation of fragmented potentials, ablation within the coronary sinus, and RA ablations were not performed. The RA isthmus was only ablated in the case of clinically documented typical RA flutter.

In patients with atrial MRT, after CT registration, activation and entrainment mapping were performed in order to identify the re-entrant circuit. The electrical information was displayed on the integrated CT surface through colour-coded isochronal lines (*Figure 5*). After the detection of the macro-re-entrant circuit and ablation of the MRT, the PVs were assessed during SR. Complete isolation of all PV funnels was performed as described earlier.

At the end of the procedure, AF/MRT inducibility was tested in all patients using 20 s Burst stimulation at the effective atrial refractory period, but did not initiate any further ablation treatment. After ablation, anti-arrhythmic drugs were discontinued and patients were put on β-blocker only. Anticoagulation was initiated for 6 months. Proton pump inhibitors were added for 4 weeks.

Following inclusion into the study and prior to ablation, a continuous 7-day electrocardiogram (ECG) (Lifecard CF, DelmarReynolds Medical Inc., Irvine, CA, USA) was recorded in all patients. The ECG was repeated immediately after the ablation and after 3 months. In the case of symptoms outside the recording periods, the patients were advised to contact our institution or the referring physician to obtain an ECG documentation. Atrial fibrillation/macro-re-entrant tachycardia longer than 30 s was considered as an episode of sustained arrhythmia recurrence. More than 27 000 h of continuous ECG recording have been analysed to assess rhythm outcome.

Statistics

Continuous variables are presented as mean ± standard deviation (SD), if appropriate. In the case of a non-Gaussian distribution,

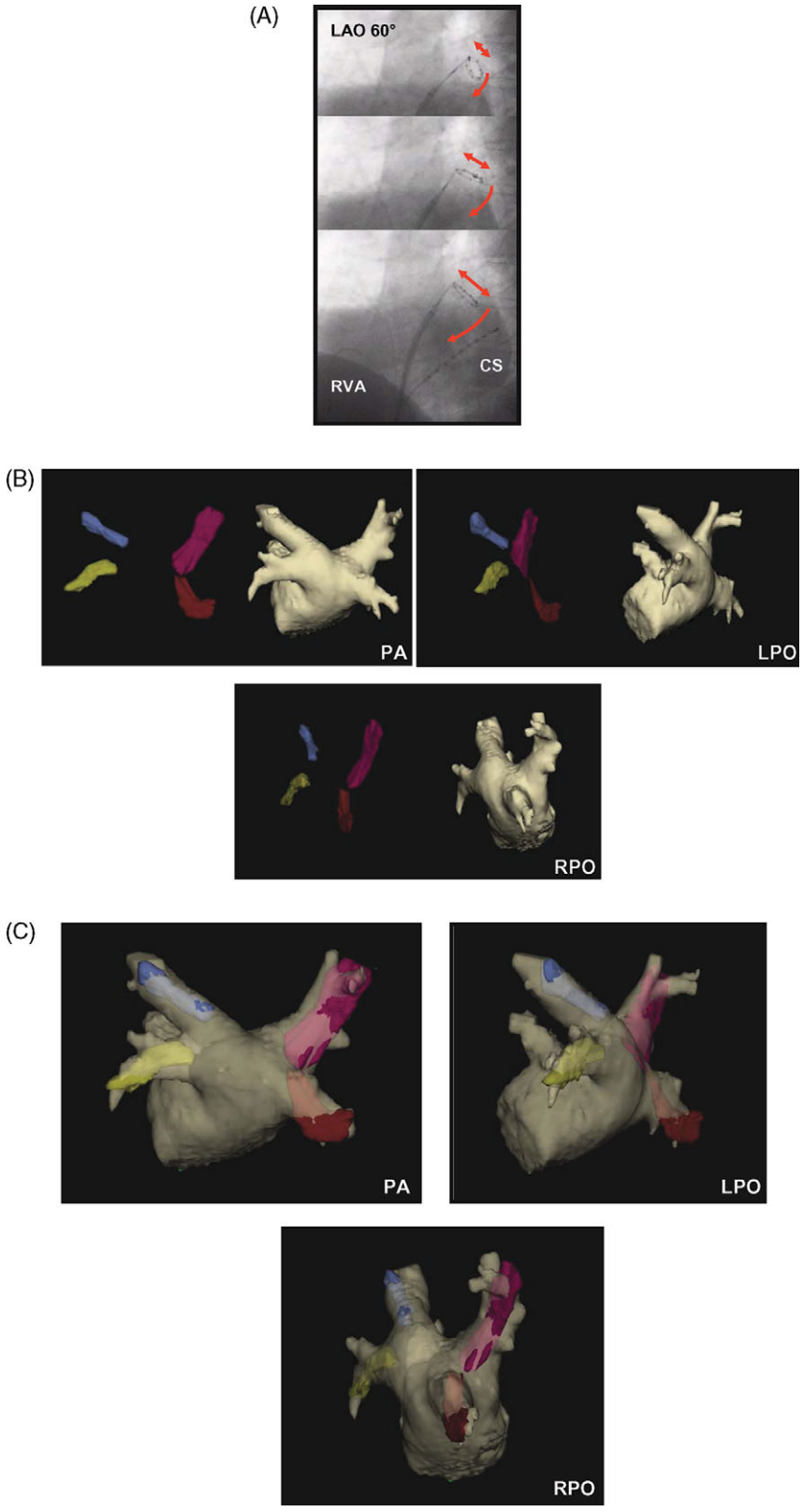

Figure 1 Main step for registering the three-dimensional computed tomography image of the left atrium into the real-time mapping system. Registration is based on reconstruction of the four pulmonary vein anatomies. (*A*) Pulmonary vein reconstruction was achieved through automatic anatomic point acquisition through all 10 poles of a multipolar circular mapping catheter while slowly withdrawing the catheter out of each pulmonary vein (in the picture, the left upper pulmonary vein). (*B*) Sync view of the four reconstructed pulmonary vein anatomies (blue, left upper pulmonary vein; yellow, left lower pulmonary vein; purple, right upper pulmonary vein; brown, right lower pulmonary vein) and the imported three-dimensional computed tomography image, before registration. (*C*) Alignment between the NavX reconstructed pulmonary vein anatomies and the pulmonary veins of the three-dimensional computed tomography image. After that main registration step, further fine adjustment was achieved through three pre-defined landmark points (left atrium roof, basal left atrium, and left atrium isthmus) visited with the ablation catheter.

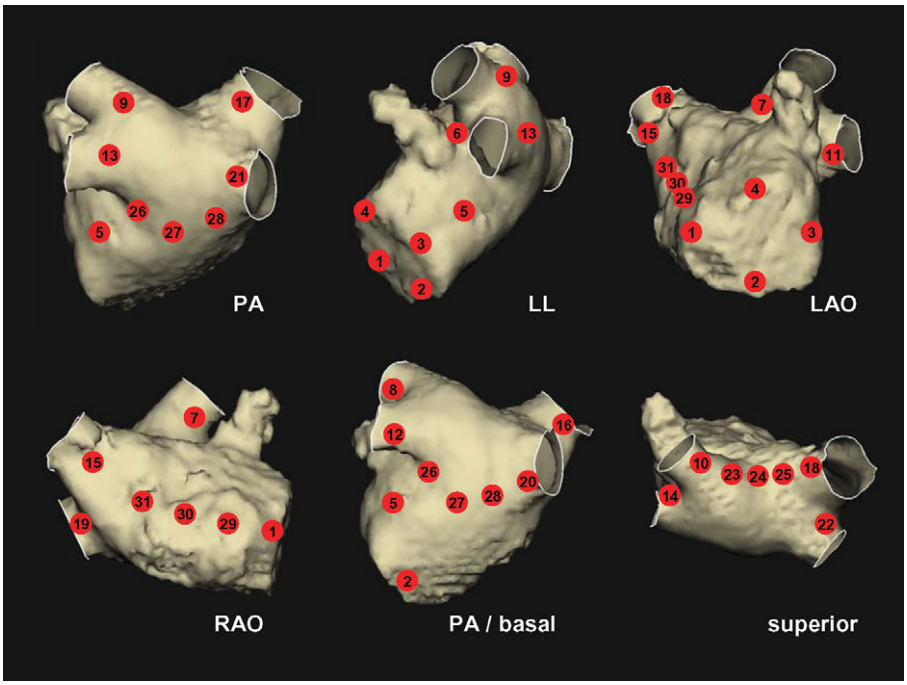

Figure 2 Control points that had to be visited with the catheter tip to assess the alignment accuracy by two independent electrophysiologists. Control point location and tissue contact were reached and assessed according to fluoroscopy information, electrogram characteristics, and tactile feedback. For each of the control points, the position of the catheter tip in relation to the registered computed tomography surface was evaluated in a nominal fashion (1–4, septal/inferior/posterior/superior mitral annulus; 5, left atrium isthmus; 6, tissue bridge between left atrium appendage and left upper pulmonary vein; 7–22, anterior/inferior/posterior/superior wall of each pulmonary vein; 23–25, left-sided, middle, and right-sided left atrium roof; 26–28, left-sided, middle, and right-sided basal left atrium; 29–31, annular, middle, and posterior part of the left atrium septum).

median and quartiles are given. Categorical variables are expressed as the number and percentage of patients.

Results

Procedural data

Mean procedure time as measured from the first femoral puncture to the removal of all sheaths was 187 ± 35 min. Registering the 3D CT into the real-time mapping system required 9 ± 3 min. Fluoroscopy time and RF burning time measured were 35 ± 12 and 47 ± 10 min, respectively. The irradiation dose was 13 800 (7200; 29 350) cGy/cm^2. In average, 45 ± 13 RF pulses were applied during the ablation.

One patient showed pericardial effusion on the post-interventional echocardiographic evaluation, which resolved after conservative treatment. Two patients developed a significant haematoma at the femoral access site without documentation of pseudoaneurysm, fistula, or deep venous thrombosis.

Table 2 displays the procedural data for the three groups of patients: paroxysmal AF, persistent AF, and atrial MRT separately.

Assessment of computed tomography alignment quality

The assessment of the 31 LA control points revealed concordance of the registered CT surface with the true catheter tip position in 90% (84%; 100%) of the control points. Thirteen patients had shown complete concordance of all control points between catheter tip and CT surface. The patient with the least accurate registration showed concordance in only 22 of 31 (71%) control points.

The quality of CT alignment was not different between patients with a newly acquired and those with a previously acquired CT scan [90% (81%; 100%) vs. 91% (84%; 100%); $P = 1.0$]. The CT alignment quality also did not differ between patients with CT imaging during SR ($n = 28$) and those with CT imaging during AF ($n = 26$) [97% (90%; 100%) vs. 94% (84%; 100%); $P = 0.827$].

The control points with the highest accuracy of the registration process and concordance between catheter tip and CT surface in all 54 patients were found within the LA isthmus; at the tissue bridge between LAA and LUPV; at the posterior wall of the LUPV; at the superior and posterior wall of the LLPV; at the superior, posterior, and inferior wall of the RUPV; at the superior wall of the RLPV; along the whole LA roof; and at the left-sided and middle parts of the basal LA. The control points with the lowest accuracy of the registration process were found at the septal mitral annulus; at the anterior wall of the RUPV; and at the annular as well as the middle aspect of the LA septum; with concordance between catheter tip and CT surface in 38 (70%), 40 (74%), 34 (63%), and 35 (65%) of the 54 patients, respectively.

During ablation, the quality of the image integration process was further verified by tagging the ablation points as '3D Lesion on EnGuide', representing the true 3D anatomical position of the catheter tip and, therefore, subjectively demonstrating the presence or the absence of contact to the integrated CT surface (*Figure 4*).

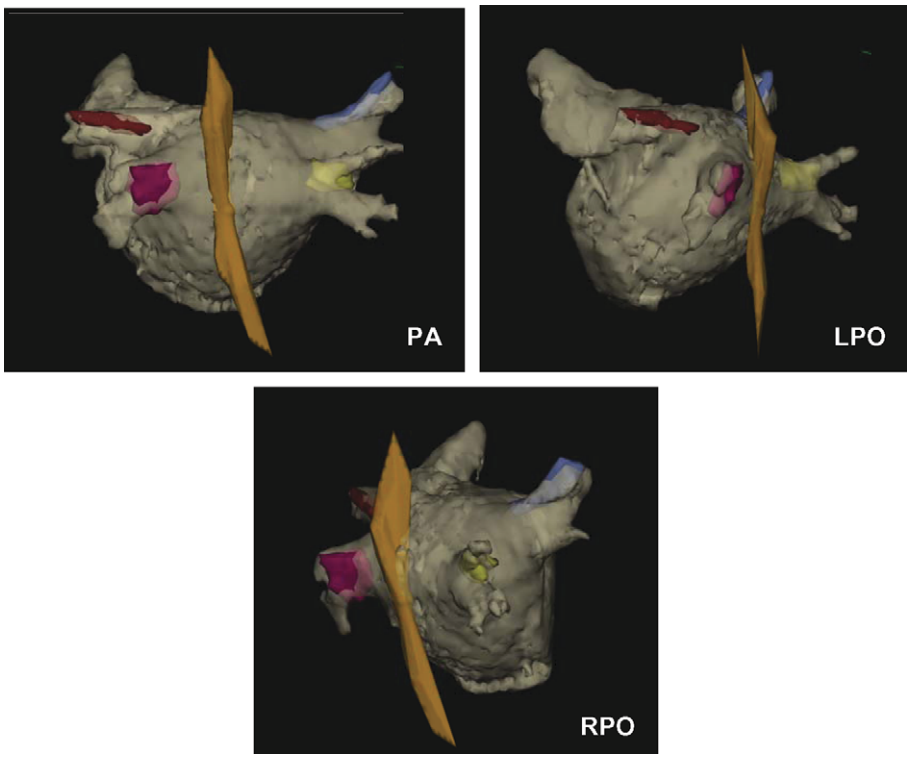

Figure 3 Following computed tomography registration and before the beginning of the ablation procedure, the oesophagus was intubated with an additional catheter, and the oesophageal anatomy was reconstructed through automatic point acquisition while slowly withdrawing the catheter out of the oesophagus. Contact and vicinity between the oesophageal anatomy reconstruction and the left atrial computed tomography anatomy was visualized. Example of a so-called B-position, where the oesophagus is positioned towards the left-sided pulmonary veins with contact at the posterior wall of the antrum of the left lower pulmonary vein (dark brown, left upper pulmonary vein; purple, left lower pulmonary vein; blue, right upper pulmonary vein; yellow, right lower pulmonary vein; light brown, oesophagus).

Ablation of atrial fibrillation

Complete isolation of the whole PV antrum for all PVs could be achieved in 35 of the 36 (97%) patients treated for AF. In 5 of the 36 (14%) patients, complete PV isolation was already found after the first placement of the circumferential ablation lines. For the remaining patients, pace and voltage mapping helped to identify and close gaps within the ablation lines. Thirty-four of the 36 (94%) patients were completely isolated before the second operator analysed the result with a multipolar mapping catheter.

Among the 11 patients presenting with persistent AF, additional isolation of the posterior LA through the placement of a roof line and a line along the basal posterior LA was successfully achieved and verified through voltage and pace mapping in all 11 patients. At the end of the procedure, aggressive Burst stimulation at the atrial refractory period was able to induce AF or MRT in 5 of the 25 patients (20%) with paroxysmal AF and 7 of the 11 patients (64%) with persistent AF (*Table 3*).

Ablation of atrial macro-re-entrant tachycardia

Of the 18 patients presenting with left atrial macro-re-entrant tachycardia (LAMRT), the re-entrant circuit could be found around the right lower PV ($n = 3$), around the left lower PV ($n = 1$), around the LUPV ($n = 2$), around the mitral annulus ($n = 4$), through the LA roof ($n = 5$), around the inter-atrial septum ($n = 2$), and around the LAA ($n = 1$). The LAMRTs around the right and left PVs were successfully treated with a circumferential LA ablation line around the ipsilateral PVs isolating the whole PV antrum (*Figure 5*). The tachycardias through the LA roof were terminated with a roof line. The perimitral re-entrant circuits were successfully treated with an ablation line in the mitral isthmus placed from endocardially ($n = 3$) and from epicardially ($n = 1$). For the septal re-entrant circuits, a linear ablation line was placed from the right PVs to the mitral annulus. The re-entrant circuit around the LAA necessitated an ablation line from the appendage towards the superior mitral annulus. After the termination of the individual LAMRT in all 18 patients, complete isolation of all PV funnels was attempted and achieved. Fifteen out of 18 (83%) patients remained non-inducible for AF and MRT on aggressive Burst stimulation at the atrial refractory period (*Table 3*).

Follow-up

Mean follow-up measured was 122 ± 33 days. In total, 8 of the 54 patients (15%) have experienced recurrences of AF and/or MRT. The following recurrences of AF and/or MRT were observed for the three groups of patients presenting with paroxysmal AF, persistent AF, and atrial MRT individually.

Two of the 18 (11%) patients presenting with atrial MRT have experienced tachycardia recurrences of MRT. Three of the 25 patients (12%) with paroxysmal AF and three of the 11 patients (27%) with persistent AF have experienced recurrences of AF.

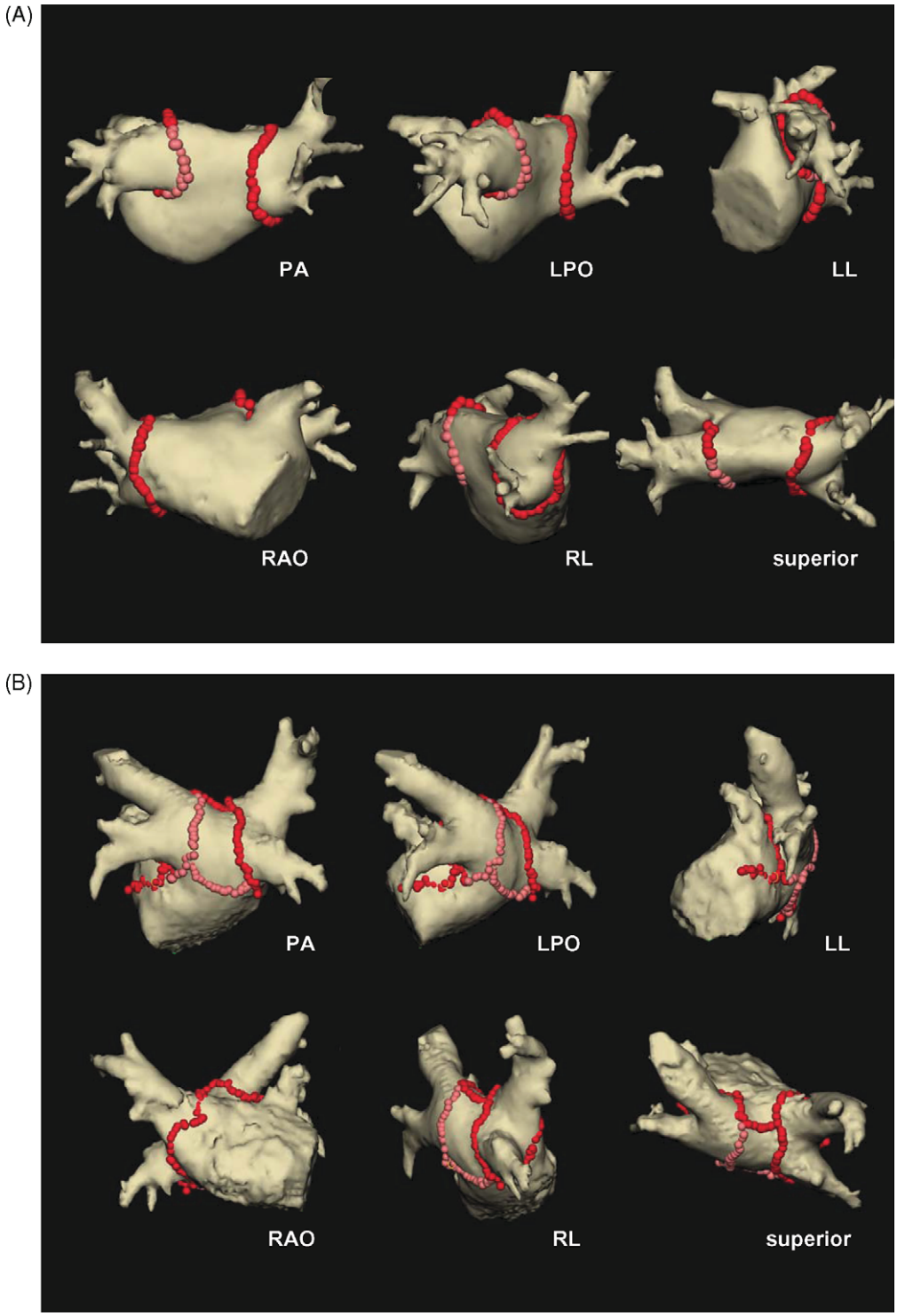

Figure 4 Left atrial ablation procedures in patients presenting with paroxysmal and persistent atrial fibrillation. Ablation points were marked as 'three-dimensional Lesion on EnGuide' (red-coloured lesion points), which documents the true three-dimensional localization of the catheter tip (no projection on computed tomography surface and no 'Lesion at Mouse'). The true position of the catheter tip on the computed tomography surface can be appreciated for all ablation target areas, underlining the registration accuracy. Pink-coloured lesion points represent ablation in areas with oesophageal vicinity (energy reduction to 30 W and shorter ablation duration). (*A*) Example of a patient with paroxysmal atrial fibrillation. Circumferential left atrial lesions were deployed around the funnels of the left- and right-sided pulmonary veins. As an anatomical variation, this patient presented with a common funnel of the left-sided pulmonary veins. (*B*) Example of a patient with persistent atrial fibrillation. After circumferential left atrial ablation, additional linear ablation lines were placed in the left atrium for further substrate modification (left atrium roof, left atrium isthmus, and posterior basal left atrium). The resulting 'box-lesion' at the posterior left atrium was completely isolated using voltage and pace mapping criteria.

Discussion

Main findings of the study

In a population of patients presenting with paroxysmal AF, persistent AF, and atrial MRT, our study shows the feasibility of successful placement of different complex linear ablation line concepts guided by an integrated 3D image anatomy alone, rather than catheter-based virtual atrial chamber reconstructions.

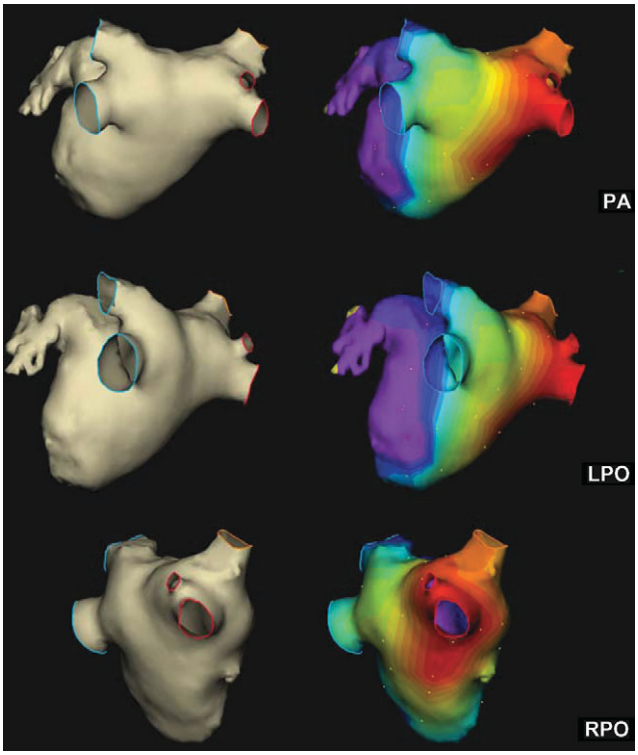

Figure 5 Example of a patient with a left atrial macro-re-entrant tachycardia. The left panel shows the pure three-dimensional computed tomography anatomy after registration. The NavX reconstructed pulmonary veins are hidden. The distal part of each pulmonary vein is cut off for image clarity. Locations within the computed tomography anatomy were visited with the ablation catheter. In stable catheter positions (small yellow points), entrainment mapping was performed. The right panel illustrates the colour-coded entrainment information in a three-dimensional fashion. Red colours representing areas with a short return cycle (close to the re-entrant circuit) and purple colours representing areas with a long return cycle (far away from the re-entrant circuit). 'Isochronal lines' connect locations with a similar length of the return cycle. The map clearly shows a macro-re-entrant circuit around the right lower pulmonary vein. Circumferential ablation around the antrum of the right-sided pulmonary veins terminated the tachycardia.

Benefits and limitations of image integration

The catheter ablation of complex atrial arrhythmias requires accurate knowledge of the true cardiac anatomy of the respective patient for the placement of either purely anatomically defined sets of ablation lines such as in those with AF or the understanding of the true 3D spread of electrical activation throughout the cardiac anatomy with subsequent design and placement of respective ablation lesions such as in patients with atrial MRT. Following that principle idea, the concept of image integration has been developed, superimposing pre-acquired 3D CT/MRI images onto the EAM chamber surface reconstruction in order to add more detailed anatomical orientation. Despite having shown clinical benefit with a higher rate of ablation success, current techniques of image integration do have limitations.[7–9] So far, registration of the pre-acquired 3D image into the real-time mapping system can be achieved with two different registration modalities—landmark and surface registration. Landmark registration is based on the alignment of distinct stable and easily accessible 3D points between the EAM surface reconstruction and their assumed position on the 3D image. For surface registration, all 3D points of the EAM surface reconstruction are attached to the closest possible CT surface. Previous studies have shown limitations for each of the two registration modalities.[10,11] Landmark registration ultimately depends on the quality of the individual landmark. Several landmarks such as aortic arch, coronary sinus, caval veins, or different LA locations have been suggested; however, registration points at the posterior PV–LA junction have resulted in the least registration error.[11] After all, although landmark registration could adequately delineate specific anatomical regions, it could not guarantee a good global fit, measured as the average distance between all 3D EAM points and the closest 3D image surface location. Surface registration, in contrast, could achieve a better global registration result; however, applying that algorithm shifted map and image significantly, dislocated well-aligned landmarks at the posterior PV–LA junction, and resulted in significant registration inaccuracies especially in target areas for circumferential PV ablation.[11] One reason for these limitations can be seen in the quality of the 3D EAM surface reconstruction, which in

Table 2 Ablation characteristics

	Paroxysmal AF ($n = 25$)	Persistent AF ($n = 11$)	MRT ($n = 18$)
Mean procedure time (min)[a]	188 ± 40	195 ± 45	205 ± 21
Mean fluoroscopy time (min)[a]	34 ± 9	45 ± 17	43 ± 12
Irradiation dose (cGy/cm^2)[b]	13 800 (11 100; 23 900)	16 200 (7100; 33 300)	15 300 (11 900; 34 000)
RF burning time (min)[b]	53 (35; 59)	61 (47; 84)	44 (31; 52)
Number of RF pulses[b]	46 (30; 60)	43 (38; 69)	37 (26; 44)
RF energy (J)[b]	97 498 (71 649; 115 680)	111 864 (98 065; 131 700)	92 416 (53 780; 980 493)

AF, atrial fibrillation; MRT, macro-re-entrant tachycardia; RF, radiofrequency.
[a]Data given as mean and standard deviation.
[b]Data given as median and quartiles.

Table 3 Procedural and clinical outcome

	Paroxysmal AF ($n = 25$)	Persistent AF ($n = 11$)	MRT ($n = 18$)
Re-entrant pathway	–	–	Perimitral (4) LA roof (5) Around PV (6) Septal (2) Around LAA (1)
Complete PV isolation, *n*(%)	24 (96)	11 (100)	18 (100)
AF/MRT inducibility, *n*(%)	5 (20)	7 (64)	3 (17)
AF/MRT recurrences, *n*(%)	3 (12)	3 (27)	2 (11)

AF, atrial fibrillation; MRT, macro-re-entrant tachycardia; LA, left atrium; PV, pulmonary vein; LAA, left atrial appendage.

itself can be anatomically misleading due to indentation of the LA wall and inadequate point collection in areas with difficult catheter access. Variations in LA size and LA anatomy due to differences in LA filling and cardiac rhythm carry further uncertainties. Owing to these limitations so far, image integration has only been used as an adjunct to conventional 3D EAM, and in questionable situations has simply been disregarded.

Image integration in the present study

Our study is the first one to report the placement of complex 3D ablation lines directly within an atrial 3D image without EAM surface reconstruction for the treatment of a larger group of patients presenting with AF and atrial MRT. Given their stable position fixated in the posterior mediastinum, the PVs served as the main registration structure (*Figure 1*).

Thirty-one pre-defined control points in the LA and at the LA–PV junction served for the assessment of the alignment quality and revealed a high accuracy of the registration process (*Figure 2*). Among all 54 patients in 90% (84%; 100%) of the control points, concordance between fluoroscopy/electrogram/tactile-guided catheter tip position and surface contact on the integrated CT image could be found. In 13 patients, all control points were imaged accurately. The highest percentage of concordance was found at the control points covering the posterior aspect of LA and PVs. The lowest percentage of concordance was found at the control points of the LA septum and anterior to the right upper PV. The fixation of the heart through the posterior LA and the PVs at the posterior mediastinum can be seen as a reason for the observed distribution of control points with higher and lower registration accuracy. The position of the posterior LA and the PVs is very stable and reproducible, which incidentally suits the purpose of AF ablation line placement. In contrast, the mitral annulus and the LA septum are much more mobile and sensitive towards changes in LA filling and cardiac rhythm, which, however, is less relevant from the point of AF catheter ablation. Optimal catheter access to all pre-defined control points and the quality of CT segmentation and 3D CT reconstruction may constitute further reasons for observed alignment inaccuracies in the mentioned areas. Clinically, in all 54 patients, the ablation procedure could be finished successfully within the CT image, and no additional atrial chamber reconstruction was required. The registration accuracy was further underlined by tagging of the ablation points as '3D Lesion on EnGuide', which technically does not represent a catheter tip projection onto the CT surface, but a true 3D position of the catheter tip revealing the presence or the absence of surface contact to the CT image (*Figure 4*).

In our approach, we did not use the Ensite Field scaling algorithm to compensate for inhomogenities in the transthoracic electrical fields. Indeed, in order to apply the field scaling algorithm, one has to first reconstruct the 3D geometry of the chamber being mapped so that the electrical field inhomogenities can be detected by non-linearities in the detected inter-electrode distances of the roving catheter. Our approach, in which the chamber is not reconstructed, therefore, does not allow the field scaling algorithm to be applied. Although the application of field scaling could lead to more accurate image integration,[12] we found our approach to be of sufficient accuracy for clinical use. Further, prospective clinical research work concerning not only the PV isolation but also the ablation of intra-atrial targets should further determine the clinical usefulness of this approach.

Patient population, procedural, and clinical outcome

Our study population included a consecutive group of patients presenting for catheter interventional treatment of AF and atrial MRT. Among them, the patients with persistent AF showed a significantly enlarged LA (53 ± 6 mm). Furthermore, 11 patients had experienced previous cardiac surgery and six patients presented with a common antrum of the left-sided PVs (*Figure 4A*).

This cohort of patients with variable and partially altered atrial anatomies presenting with different types of complex atrial arrhythmias rather constitutes a challenge for the interventional electrophysiologist. However, in all patients, it was possible to plan and perform the required lesion line concept within the anatomy of the registered 3D image without atrial chamber reconstruction.

In all 54 patients complete isolation of all PVs was attempted. In patients with AF that was the primary therapeutical target. In patients with MRT, the primary therapeutical target was to map, and ablate the MRT, but afterwards as a secondary therapeutical target the PVs were also isolated in those patients. In 53 of the 54 (98%) patients, complete isolation was achieved and verified through bidirectional block on a circular multipolar mapping catheter placed by a second electrophysiologist who was not involved in the ablation part of the procedure.

On a follow-up based on a serial 7-day-Holter ECG including the analysis of more than 27 000 h of ECG recording, the clinical outcome showed 88% freedom from AF and/or MRT in patients presenting with paroxysmal AF. In patients with persistent AF, the success rate (freedom from AF and/or MRT) after a single LA intervention measured 73%. Sixteen of 18 (89%) patients presenting with atrial MRT remained free of AF and/or MRT during follow-up.

Limitation of the study

Our study, although being prospective in nature, represents a non-randomized single-centre experience. The current follow-up period does not allow a final judgement on long-term clinical benefit; however, the main purpose of the study was to analyse procedural aspects with a clear electrophysiologically defined procedural endpoint.

The assessment of the accuracy of 3D image integration *in vivo* is difficult, given a moving organ, a breathing patient, and a static image. Imaging modalities such as MRI or intra-cardiac echo lack spatial resolution or 3D orientation to provide an accurate *in vivo* assessment of 3D image integration accuracy. We therefore took a very clinical approach and validated the position of the tip of the catheter within the integrated CT image against our judgement on catheter tip position derived from fluoroscopy, local electrogram, and tactile information. This is a rough and non-quantitative assessment. However, performed for 31 different points throughout the LA and the PV individually, it does give a good impression as to whether the registration is accurate and the catheter appears in the CT where we would expect it to or whether this is not the case.

Furthermore, potential inaccuracies in the control point analysis result from changes in LA filling, cardiac cycle length, and respiratory motion.

Clinical implications

Our study describes practical image integration in one of the most widely used electro-anatomical mapping systems, NavX-Ensite. Utilizing this tool, feasibility of successful placement of different complex linear ablation line concepts guided by an integrated 3D image anatomy alone, rather than catheter-based virtual chamber reconstructions, has been shown in a heterogeneous group of patients presenting with a variety of atrial anatomies and clinical arrhythmias.

Following the principle idea, that a 3D reconstructed imaging technology provides higher anatomical accuracy when compared with any virtual point-by-point EAM surface reconstruction, our data are part of the first steps to develop approaches, in which electrophysiological analysis, therapy planning, and ablation can be performed within realistic 3D cardiac chamber anatomies. Currently, CT scan radiation exposures and off-line CT segmentation represent limitations for that concept. However, 3D images acquired on-line during the EP procedure (through either rotation angiography or even echocardiography), and immediately exported into the real-time mapping system, may develop into simple tools to overcome these limitations.

Conflict of interest: none declared.

Funding

Funding to pay the Open Access publication charges for this article was provided by Hospital resources.

References

1. Ben-Haim SA, Osadchy D, Schuster I, Hayam G, Josephson ME. Nonfluoroscopic, *in vivo* navigation and mapping technology. *Nat Med* 1996;**2**:1393–5.
2. Krum D, Goel A, Hauck J, Schweitzer J, Hare J, Attari M *et al*. Catheter location, tracking, cardiac chamber geometry creation, and ablation using cutaneous patches. *J Interv Card Electrophysiol* 2005;**12**:17–22.
3. Piorkowski C, Hindricks G, Schreiber D, Tanner H, Weise W, Koch A *et al*. Electroanatomic reconstruction of the left atrium, pulmonary veins, and esophagus compared with the 'true anatomy' on multislice computed tomography in patients undergoing catheter ablation of atrial fibrillation. *Heart Rhythm* 2006;**3**:317–27.
4. Dong J, Dickfeld T, Dalal D, Cheema A, Vasamreddy CR, Henrikson CA *et al*. Initial experience in the use of integrated electroanatomic mapping with three-dimensional MR/CT images to guide catheter ablation of atrial fibrillation. *J Cardiovasc Electrophysiol* 2006;**17**:459–66.
5. Kistler PM, Rajappan K, Jahngir M, Earley MJ, Harris S, Abrams D *et al*. The impact of CT image integration into an electroanatomic mapping system on clinical outcomes of catheter ablation of atrial fibrillation. *J Cardiovasc Electrophysiol* 2006;**17**:1093–101.
6. Shalganov TN, Vatasescu R, Paprika D, Kornyei L, Vanyi J, Geller L *et al*. A simple algorithm for defining the mechanism and the chamber of origin in atrial tachycardias. *J Electrocardiol* 2006;**39**:369–76.
7. Kottkamp H, Piorkowski C, Tanner H, Kobza R, Dorszewski A, Schirdewahn P *et al*. Topographic variability of the esophageal left atrial relation influencing ablation lines in patients with atrial fibrillation. *J Cardiovasc Electrophysiol* 2005;**16**:146–50.
8. Heist EK, Chevalier J, Holmvang G, Singh JP, Ellinor PT, Milan DJ *et al*. Factors affecting error in integration of electroanatomic mapping with CT and MR imaging during catheter ablation of atrial fibrillation. *J Interv Card Electrophysiol* 2006;**17**:21–7.
9. Ferguson J. Optimizing catheter navigation for AF ablation: do not just follow the map!. *J Cardiovasc Electrophysiol* 2007;**18**:283–5.
10. Zhong H, Lacomis JM, Schwartzman D. On the accuracy of CartoMerge for guiding posterior left atrial ablation in man. *Heart Rhythm* 2007;**4**:595–602.
11. Fahmy TS, Mlcochova H, Wazni OM, Patel D, Cihak R, Kanj M *et al*. Intracardiac echo-guided image integration: optimizing strategies for registration. *J Cardiovasc Electrophysiol* 2007;**18**:276–82.
12. Brooks AG, Wilson L, Kuklik P, Stiles MK, John B, Hany Dimitri S *et al*. Image integration using NavX Fusion: initial experience and validation. *Heart Rhythm* 2008;**5**:526–35.